Oncology Research, Vol. 28, pp. 451–465
Printed in the USA.

0965-0407/20 $90.00 + .00
DOI: https://doi.org/10.3727/096504020X15898794315356
E-ISSN 1555-3906
www.cognizantcommunication.com

Pivarubicin Is More Effective Than Doxorubicin Against Triple-Negative Breast Cancer In Vivo

Leonard Lothstein,* Judith Soberman,† Deanna Parke,* Jatin Gandhi,*
Trevor Sweatman,‡ and Tiffany Seagroves*

*Department of Pathology and Laboratory Medicine, The University of Tennessee Health Science Center, Memphis, TN, USA
†Department of Medicine, The University of Tennessee Health Science Center, Memphis, TN, USA
‡Department of Pharmacology, The University of Tennessee Health Science Center, Memphis, TN, USA

Triple-negative breast cancer (TNBC) is unresponsive to antiestrogen and anti-HER2 therapies, requiring the use of cytotoxic drug combinations of anthracyclines, taxanes, cyclophosphamide, and platinum compounds. Multidrug therapies achieve pathological cure rates of only 20–40%, a consequence of drug resistance and cumulative dose limitations necessitated by the reversible cardiotoxic effects of drug therapy. Safer and more effective treatments for TNBC are required to achieve durable therapeutic responses. This study describes the mechanistic analyses of the novel anthracycline, pivarubicin, and its in vivo efficacy against human primary TNBC. Pivarubicin directly activates PKCd, triggers rapid mitochondrial-dependent apoptosis, and circumvents resistance conferred by overexpression of P-glycoprotein, Bcl-2, Bcl-X_L, and Bcr-Abl. As a consequence, pivarubicin is more cytotoxic than doxorubicin against MDA-MB-231, and SUM159 TNBC cell lines grown in both monolayer culture and tumorspheres. Comparative in vivo efficacy of pivarubicin and doxorubicin was performed in an orthotopic NSG mouse model implanted with MDA-MB-231 human TNBC cells and treated with the maximum tolerated doses (MTDs) of pivarubicin and doxorubicin. Tumor growth was monitored by digital caliper measurements and determination of endpoint tumor weight and volume. Endpoint cardiotoxicity was assessed histologically by identifying microvacuolization in ventricular cardiomyocytes. Primary tumors treated with multiple rounds of doxorubicin at MTD failed to inhibit tumor growth compared with vehicle-treated tumors. However, administration of a single MTD of pivarubicin produced significant inhibition of tumor growth and tumor regression relative to tumor volume prior to initiation of treatment. Histological analysis of hearts excised from drug- and vehicle-treated mice revealed that pivarubicin produced no evidence of myocardial damage at a therapeutic dose. These results support the development of pivarubicin as a safer and more effective replacement for doxorubicin against TNBC as well as other malignancies for which doxorubicin therapy is indicated.

Key words: Pivarubicin; Doxorubicin; Apoptosis; Triple-negative breast cancer (TNBC); Chemotherapy; Cardiotoxicity

INTRODUCTION

Triple-negative breast cancer (TNBC) is a highly aggressive subtype that neither expresses estrogen receptors (ERs) and progesterone receptors nor overexpresses epidermal growth factor 2 receptor (HER2). As a consequence, TNBC is unresponsive to antiestrogen and anti-HER2 therapies and is treated with systemic cytotoxic drug combinations of anthracyclines, such as doxorubicin, taxanes, cyclophosphamide, and platinum compounds[1–3]. More targeted therapies are undergoing clinical trials[4]. Despite initial sensitivity to chemotherapy, TNBC patients experience lower overall disease-free intervals compared with patients whose tumors express sex steroid hormone receptors[5], with an overall pathological complete response (pCR) of only 20–40%[6]. The limited cytotoxic efficacy of chemotherapy is likely due to multiple mechanisms of drug resistance, as well as cell senescence and cytoprotective autophagy[1]. Further, the irreversible cardiotoxic effects of anthracyclines and, to a lesser extent, other chemotherapeutics are well established and limit the cumulative doses of drugs that can be administered to achieve a curative outcome[7,8].

Address correspondence to Leonard Lothstein, Ph.D., Department of Pathology and Laboratory Medicine, University of Tennessee Health Science Center, 19 S. Manassas St., Memphis, TN 38163, USA. Tel: 901-448-3334; E-mail:llothstein@uthsc.edu

Therefore, a critical unmet need exists for safer and more effective treatments for TNBC that eliminate drug-resistant cell subpopulations without producing cardiotoxicities, thereby reducing the probability of recurrent disease and irreversible cardiac damage. *N*-Benzyladriamycin-14-pivalate (pivarubicin; AD 445) was designed and developed as a chemically stable congener of the experimental antitumor agent *N*-benzyladriamycin-14-valerate (AD 198)[9]. AD 198 had been previously shown to competitively bind to the C1b (diacylglycerol binding) regulatory domain of conventional and novel isoforms of protein kinase C (PKC) in the cytoplasmic compartment of mammalian cells[10–12]. AD 198 is functionally distinct from doxorubicin in its ability to trigger rapid, mitochondrial-dependent apoptosis through PKC-delta (PKCd) activation in a manner that circumvents multiple mechanisms of cellular drug resistance[12–16]. Further, through the specific activation of PKCe in mammalian cardiomyocytes, AD 198 confers cardioprotection against reperfusion injury following global ischemia and doxorubicin-induced cardiac damage[17,18]. However, AD 198 is labile to rapid ester hydrolysis of the valerate moiety, resulting in the formation of *N*-benzyladriamycin (AD 288), a catalytic inhibitor of topoisomerase II with reduced ability to circumvent resistance mediated by multidrug transport proteins or antiapoptotic protein overexpression[12,19].

In this study, we will confirm the stability of the tertiary trimethylester moiety of pivarubicin against hydrolysis and determine whether: 1) pivarubicin rapidly triggers apoptosis in a PKCd-dependent manner, 2) these functional characteristics confer therapeutic superiority to pivarubicin over doxorubicin using an orthotopic xenograft model of the aggressive MDA-MB-231-LM2 human TNBC cells implanted in immunodeficient NSG mice, and 3) TNBC tumor growth inhibition by pivarubicin is achieved in the absence of histological evidence of cardiac damage.

MATERIALS AND METHODS

Chemicals and Biologicals

Pivarubicin, originally designed by Dr. Mervyn Israel (University of Tennessee Health Science Center, Memphis, TN, USA), was synthesized by Dr. John Rimoldi (University of Mississippi, Oxford, MS, USA) using a previously described protocol[20,21]. Doxorubicin HCl, rottlerin, and all antibodies were purchased from Sigma-Aldrich (St. Louis, MO, USA). For in vitro experiments, doxorubicin and pivarubicin were dissolved in dimethyl sulfoxide (DMSO). The final maximum DMSO concentration used for in vitro drug treatments (1% for 72 h) was not cytotoxic. IL-3-dependent 32D.3 murine myeloid cells, CCRF-CEM human lymphoblastic leukemia cells and multidrug-resistant variants (generous gift of Dr. William T. Beck, St. Jude Children's Research Hospital, Memphis, TN, USA), 293 embryonic human kidney cells and HL-60 human acute myeloid leukemia cells transfected with Bcr-Abl, Bcl-X_L, or empty expression vectors (generous gift of Dr. Kapil Bhalla, University of Miami, Coral Gables, FL, USA) were maintained as previously described[12,14,22,23]. K562 human chronic myelogenous leukemia and LNCaP human prostate cancer cells were purchased from ATCC (Manassas, VA, USA) and maintained as described by the vendor. LNCaP/Bcl-2 cells were the generous gift of Dr. Ralph Buttyan (Columbia University, New York City, NY, USA). Luminescent MDA-MB-231-LM2 (LM-2; metastatic lung subpopulation isolated from human TNBC MDA-MB-231 cells transduced with eIF1a-Luc2-puro lentivirus) were generously provided by Dr. Yibin Kang (Princeton University, Princeton, NJ, USA) and maintained in culture as previously described[24]. PKCd siRNA[25] and scrambled variant were obtained from Qiagen (Hilden, NRW Germany).

Drug Biotransformation Analysis

Quantitative and qualitative determination of AD 198 and pivarubicin biotransformation was determined by reversed-phase HPLC as described previously[26,27].

Fluorescence Microscopy

32D.3 cells were grown in suspension culture in the absence of a drug for 24 h prior to analysis. Cells at a density of 1×10^6/ml were exposed to 5 μM doxorubicin or 1 μM pivarubicin for 1 h and then harvested, washed, and resuspended in phosphate-buffered saline, pH-7.2 (PBS). Nuclear counterstaining of pivarubicin-treated cells was performed by treatment of cells with 16 μg/ml of bisbenzimide for 1 h. Drug autofluorescence was observed with an Olympus BH-2 phase-contrast microscope with a mercury UV light source under UV illumination (red: excitation filter, 530–560 nm; barrier filter, 580 nm; blue: excitation filter, 340–390 nm) at a magnification of 1,000×.

Analysis of Apoptosis

Detection of DNA fragmentation in apoptotic cells by the TUNEL assay and immunoblot analyses of cytochrome c release were performed as described previously[12].

PKC Inhibition, Cell Viability Determinations, and Immunoblot Analysis

Rottlerin treatment of cells, cell viability analysis by MTT[28], and immunoblot identification of protein expression were performed and described previously[12].

Injection of Cells Into the Murine Mammary Fat Pad

Monolayer LM2 cells were trypsinized and resuspended in DMEM media containing 10% FBS and 1×

antibiotic/antimitotic. Cell concentration was adjusted to yield 2.5×10^5 cells for each 10-µl injection in PBS. After preparation for injection, cells were kept on ice at all times. Cells were surgically implanted into the left and right inguinal mammary glands of 4-week-old female NSG mice (NOD/SCID IL2R$\gamma^{-/-}$; #5557; Jackson Laboratory, Bar Harbor, ME, USA) bred in-house. Mice were anesthetized with 1.2% avertin via intraperitoneal (IP) injection prior to surgery. Mice were also injected subcutaneously between shoulder blades with rimadyl for pain relief on the day of surgery and on the day following surgery. Primary tumor growth prior to and during drug treatment was monitored initially by manual palpation for tumor appearance, then twice weekly using digital calipers. Tumor volume was calculated by the formula: volume = (width^2 × length)/2. When tumors attained a volume of approximately 150–190 mm^2, cohorts of 10 randomized drug-naive, female NSG mice (8 ± 1 weeks old, 23 ± 2 g) were administered the maximum tolerated dose (MTD) of pivarubicin, doxorubicin, or the equivalent volume of vehicle (70% sterile saline, 15% ethanol, 15% Cremophor EL) as a bolus IP injection in parallel experiments. Tumor volumes were measured in a blinded manner. All mice were maintained on a 7904-irradiated high-fat diet (Teklad, Madison, WI, USA). Food/water was provided ad libitum. Animal health was monitored by visual observation supplemented by body condition scoring as well as weight loss to monitor endpoint (greater than 20%) measured two to three times/week. All animal procedures were approved by the Institutional Animal Care and Use Committee at the University of Tennessee Health Science Center as accredited by the Association for the Assessment and Accreditation of Laboratory Animal Care.

At termination of experiments, mice were sacrificed humanely by CO_2 inhalation followed by cervical dislocation.

Imaging Mice Using In Vivo Imaging System

Mice were imaged using Xenogen In Vivo Imaging System® Lumina from PerkinElmer (Waltham, MA, USA). Stock D-luciferin firefly potassium salt (122799; Perkin Elmer) was prepared in Dulbecco's-PBS (DPBS) at a concentration of 30 mg/ml and sterile filtered with 0.2-µm syringe filter. Luciferin was further diluted to 15 mg/ml in DPBS prior to injection. Mice were injected IP with 200 µl of luciferin. Primary tumors were imaged by placing the mice in dorsal recumbency using luminescent setting of auto exposure, field of view D with a resolution setting of 4 (medium binning), 10 min after injection with luciferin, approximately 5 min following anesthetization with isoflurane. Data are reported as total flux in photons per second (p/s) using the Living Image software.

Cardiotoxicity Assessment

Drug-mediated cardiotoxicity was assessed in both nontumor-bearing female NSG mice administered three doses (IP every 2 weeks) of the MTD of doxorubicin, pivarubicin, or the equivalent volume of solvent only and in hearts excised from tumor-bearing mice treated as described in the Results section. Body weights were monitored every 3 days. Two weeks after the final dose, mice were sacrificed, and the hearts were excised immediately. Intact ventricular myocardia were fixed for a minimum of 24 h in 10% formalin phosphate buffered to pH 7.0 and then carefully sectioned into 2- to 3-mm-thick slices before being dehydrated in graded ethanol and cleared in xylene prior to embedding in paraffin at 58°C. Sections (4-µm thick) were mounted on glass slides, deparaffinized in xylene, and stained in the routine fashion with Mayer's hematoxylin and eosin. Slide labels were blinded to evaluator. Myocardial lesions were evaluated by routine light microscopy and scored with regard to the severity and extent of damage[29]:

> *Degree of severity* (*S*)—0, no evidence of histological changes; 1, sarcoplasmic microvacuolization and/or inclusions (interstitial or cellular edema); 2, as in 1 plus sarcoplasmic macrovacuolization or atrophia, necrosis, fibrosis, endocardial lesions, and thrombi.
>
> *Degree of extension* (*E*)—0, no lesions; 0.5, less than 10 single altered myocytes on the whole-heart section; 1, scattered single altered myocytes; 2, scattered small groups of altered myocytes; 3, spread small groups of altered myocytes; 4, confluent groups of altered myocytes; 5, most of cells damaged.
>
> *Total cardiotoxicity score/animal* = $S \times E$, and mean total score (MTS) for each treatment group was MTS = $\sum(S \times E)$/number of animals.

RESULTS

Pivarubicin was designed to be a hydrolytically stable congener of our previously developed anthracycline antitumor compound, AD 198. In contrast to the straight-chain five-carbon valerate moiety at C-14 appended to the anthraquinone A ring through an esterase-labile ester linkage in AD 198, pivarubicin contains a tertiary trimethylester (pivalate) moiety that likely sterically hinders enzyme-mediated ester hydrolysis, yet retains the three-dimensional configuration that mimics the C1b regulatory domain ligands, diacylglycerol and phorbol 12-myristate 13-acetate[11] (Fig. 1). Resistance of the pivalate moiety to hydrolysis is confirmed following treatment of multiple mammalian cell lines with pivarubicin and AD 198, followed by qualitative and quantitative analysis of drug content by reversed-phase HPLC[26,27]. While AD 198 is subject to approximately 50% biotransformation to *N*-benzyladriamycin (AD 288) 8 h after drug uptake into cells, less than 10% of pivarubicin is initially

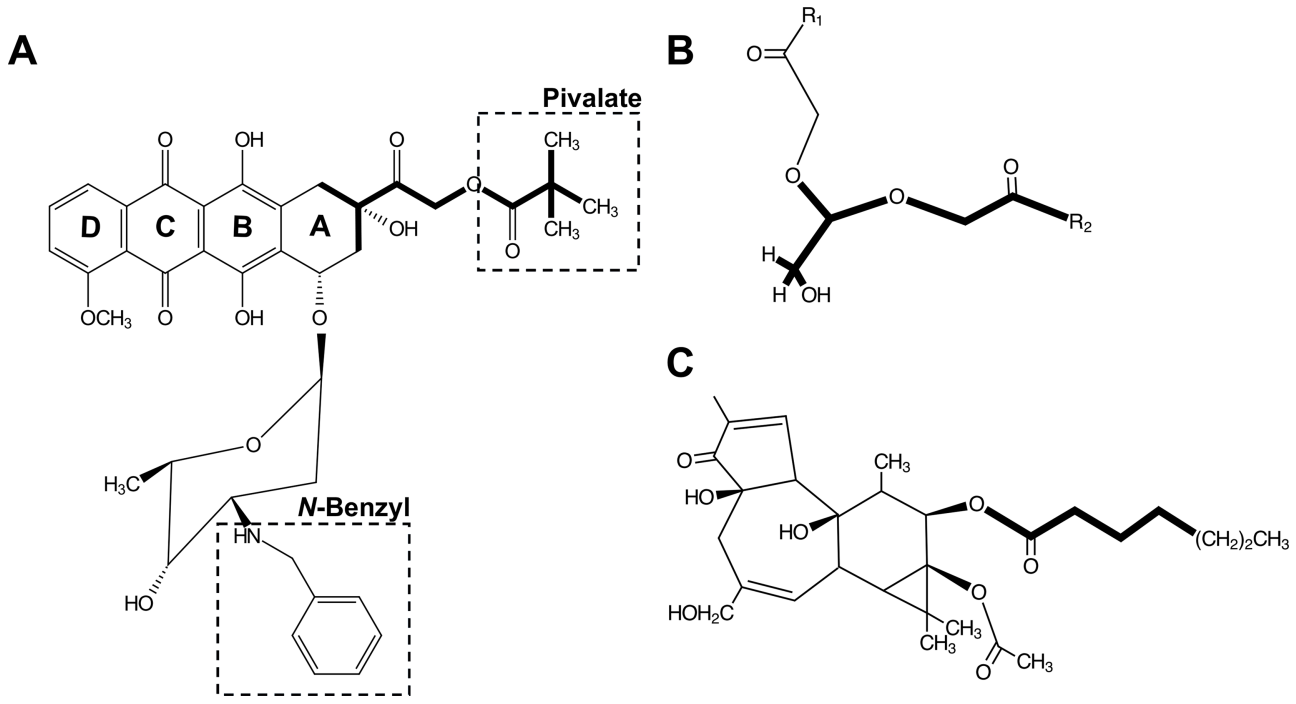

Figure 1. Isosteric similarity of pivarubicin and diacylglycerol (DAG). Bold lines identify the putative pharmacophores (C1b binding site) for (A) pivarubicin, (B) diacylglycerol (DAG), and (C) phorbol 12-myristate 13-acetate (PMA).

biotransformed and shows little time-dependent conversion to AD 288 (Table 1).

By possessing a hydrolytically stabile C-14 moiety, we determined the functional characteristics of pivarubicin in cell types (CCRF-CEM, 32D.3, LNCaP, HL-60) that were used in the previous mechanistic analyses of AD 198[12–14] to determine if hydrolytic stability altered the function of pivarbicin compared with AD 198. As predicted, pivarubicin retains the functional characteristics initially described for AD 198, including rapid cellular uptake and localization almost exclusively in the perinuclear region of the cytoplasm (Fig. 2). Once distributed into microsomal membranes, pivarubicin triggers rapid, mitochondrial-dependent apoptosis that is independent of cell cycle arrest (Fig. 3). Marked release of cytochrome c into the cytosol as an indicator of mitochondrial depolarization and dysfunction is detected within 5 h of drug treatment, while DNA fragmentation, as detected by TUNEL staining, is abundant by 6 h.

Table 1. Esterase Resistance of Pivarubicin

	% Parent Compound					
	32D.3		293		J774.2	
	1 h	8 h	1 h	8 h	1 h	8 h
AD 198*	90%	56%	80%	50%	90%	50%
Pivarubicin*	100%	96%	98%	94%	90%	90%

*1 μM drug at 37°C for 1 h/7 h in drug-free medium.

Consistent with the computer modeling and binding studies of *N*-benzylanthracyclines with varying C-14 acyl chain length and conformation with the C1b regulatory of PKC[10,11], pivarubicin-induced cytotoxicity is dependent on PKCd activation (Fig. 4). Within 4 h of treatment with 5 μM pivarubicin, PKCd translocates from the cytosolic to the membrane cellular fraction, consistent with PKCd activation (Fig. 4A). Consistent with this finding, inhibition of PKCd activity also selectively impedes pivarubicin cytotoxicity. Treatment of cells with the IC_{50} concentration of doxorubicin produces a progressive decrease in the viable cell population down to 50% by 24 h of drug treatment. Cotreatment of cells with rottlerin, a selective inhibitor of the proapoptotic PKCd, does not alter doxorubicin cytotoxicity. However, while pivarubicin produces 50% cell kill within 6 h of treatment, rottlerin markedly delays pivarubicin 50% cell kill to 24 h (Fig. 4B). Likewise, downregulation of PKCd expression in human LNCaP prostate cancer cells by PKCd siRNA transfection inhibits pivarubicin-mediated cell kill, with a 2.5-fold increase in pivarubicin concentration required to achieve 50% cell kill in PKCd–siRNA-transfected cells, thus supporting PKCd activation by pivarubicin as the trigger for apoptosis (Fig. 4C).

In addition to its novel mechanisms of cytotoxic action, pivarubicin circumvents multiple mechanisms of cellular

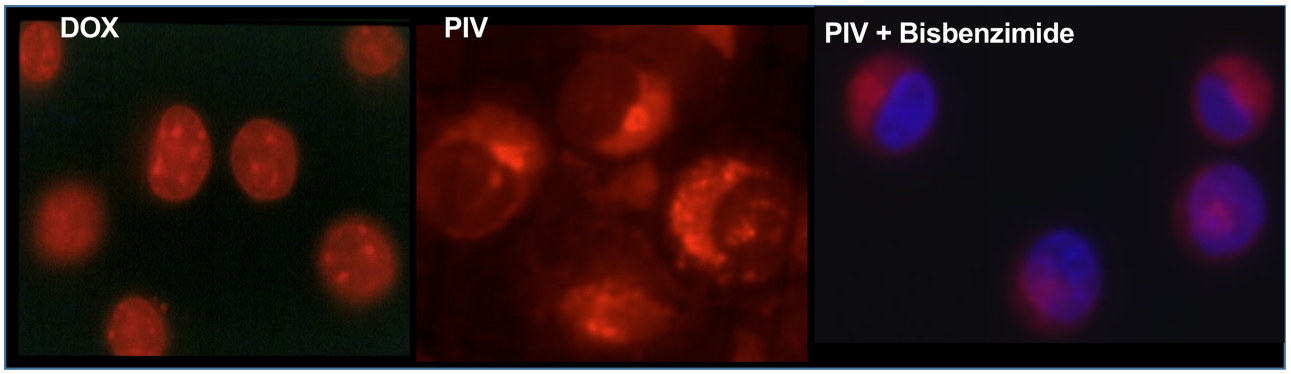

Figure 2. Cellular localization of pivarubicin. 32D.3 cells at a density of 1×10^6/ml were exposed to 5 μM doxorubicin or 1 μM pivarubicin for 1 h. Nuclear counterstaining of pivarubicin-treated cells was performed with 16 μg/ml of bisbenzimide for 1 h. Fluorescence microscopy was performed as described in the Materials and Methods section. Images' original magnification: 1,000×.

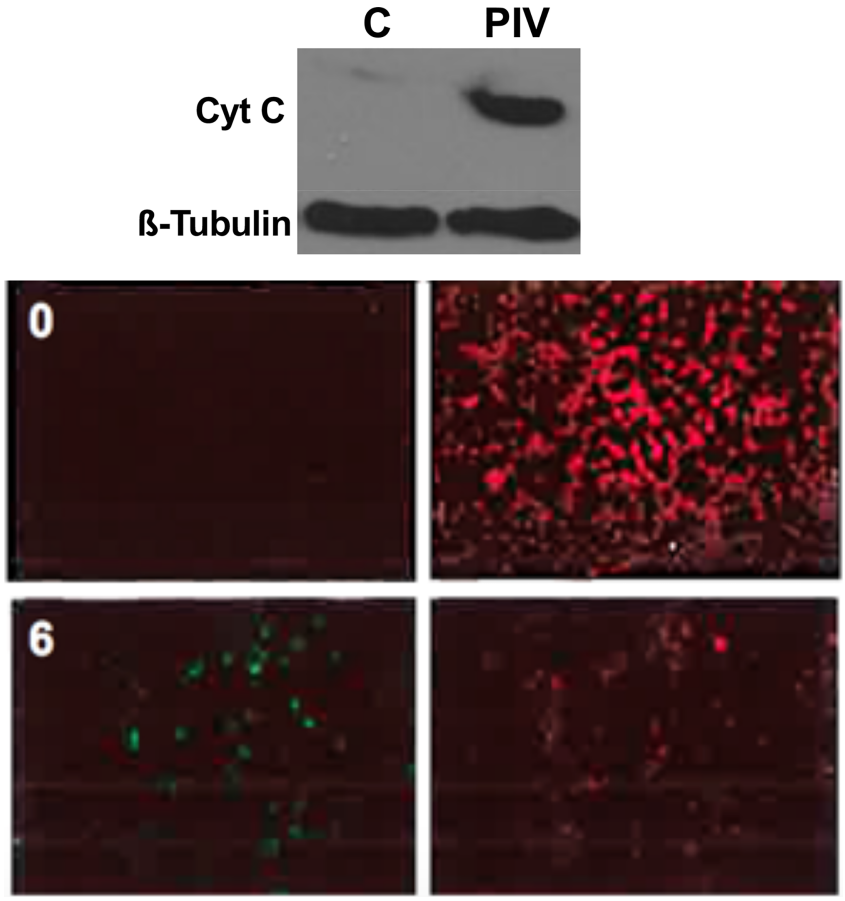

Figure 3. Pivarubicin-mediated rapid apoptosis. (A) Cytochrome c release by pivarubicin. 32D.3 cells were exposed to 5 μM pivarubicin for 1 h and then incubated in drug-free medium for an additional 4 h. Cells were then fractionated to isolate the cytosolic fraction, subjected to immunoblotting, and treated with anti-cytochrome c monoclonal antibody (1:250) for 2 h, followed by a 1-h treatment with 1:1,000 dilution of horseradish peroxidase-conjugated goat anti-mouse second antibody as described previously[12]. Proteins were detected by chemiluminescence. (B) Detection of DNA fragmentation in pivarubicin-treated 32D.3 cells by TUNEL assay. Cells were treated with 5 μM pivarubicin for 1 h, washed twice in warm PBS, incubated in drug-free medium for 6 h, and then prepared for 3′-biotinylation of fragmented DNA using the TUNEL assay procedure. Individual fields of cells were detected for both DNA 3′-end labeling (green) or total cellular DNA staining by propidium iodide (red). Composite image is representative of three independent experiments.

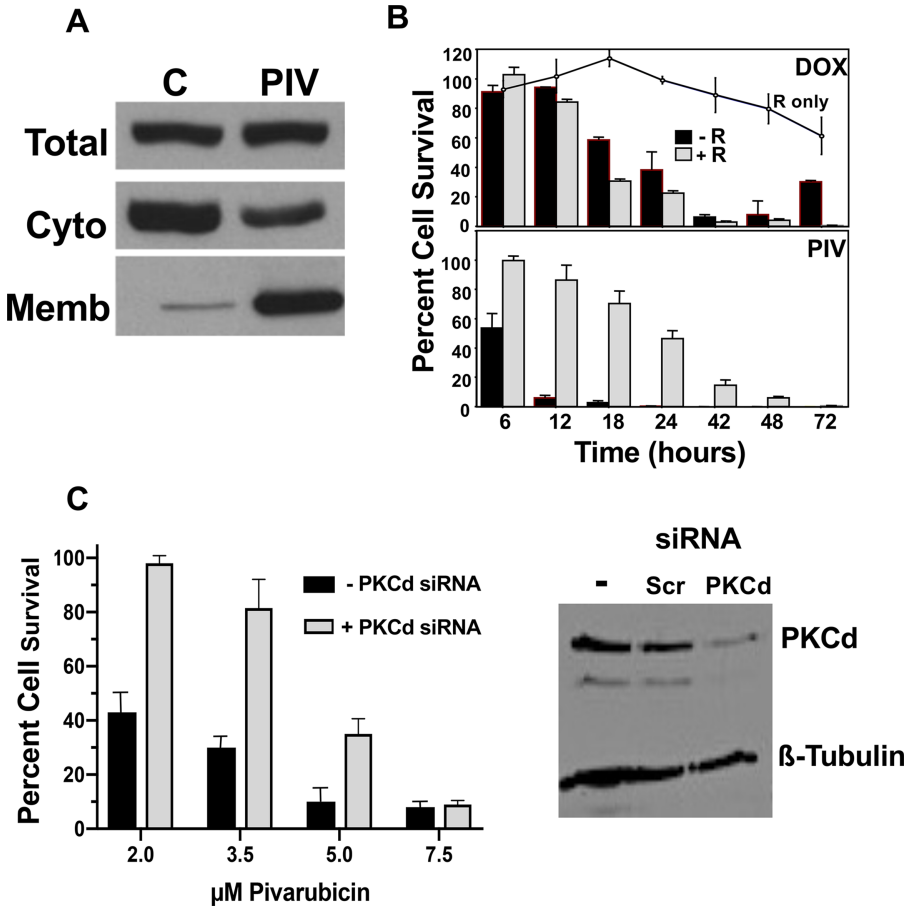

Figure 4. Pivarubicin cytotoxicity is mediated through PKC-delta (PKCd) activation. (A) 32D.3 cells, suspended in RPMI-1640 medium/10% FCS/IL-3 at a density of 5×10^5 cells/ml, were treated with either DMSO (C) or 5 µM pivarubicin (PIV) for 4 h prior to harvesting, cell fractionation, and immunoblot analysis of PKCd as described previously[14]. (B) 32D.3 cells were pretreated with 10 µM rottlerin for 2 h prior to exposure to 5 µM drug for 1 h at 37°C. Cells were pelleted and washed twice in large volumes of warm PBS, then resuspended in fresh, drug-free medium containing 10 µM rottlerin at 5×10^5 cells/ml and incubated at 37°C for up to 72 h. At indicated times, aliquots of cells were withdrawn and stained with trypan blue. Viable cells were scored based on the exclusion of stain and gross morphological appearance. (C) 32D.3 cells were transfected with PKCd siRNA or scrambled siRNA as described in the Materials and Methods section and assessed for pivarubicin cytotoxicity as in (A). Each datum point represents the mean and standard error of at least three independent determinations, each consisting of 300–500 cells per count, when possible.

drug resistance. CCRF-CEM cells selected for resistance to vinblastine (CEM/VLB-10 and CEM/VLB-100) overexpress P-glycoprotein, exhibit 10.6- and 269-fold resistance to vinblastine[22], and exhibit 12- and 73-fold resistance to doxorubicin, respectively. However, VLB-10 cells exhibit no resistance to pivarubicin, and VLB-100 cells are only threefold resistant. Overexpression of transfected antiapoptotic proteins Bcl-2 in LNCaP human prostate cancer cells (Fig. 5A) and Bcl-X_L in HL-60 human promyelocytic leukemia cells (Fig. 5B) does not impede the rate of pivarubicin-induced apoptosis. Further, the oncogenic fusion protein, Bcr-Abl, had no inhibitory effect on pivarubicin cytotoxicity in HL-60 cells, in contrast to doxorubicin (Fig. 5B). In total, these cell-based results indicate that, similar to its more chemically labile congener, AD 198, the rapid uptake of pivarubicin in mammalian cells, which is unaffected by P-glycoprotein expression, results in cytoplasmic localization of drug, and rapid translocation and activation of PKCd to trigger mitochondrial-dependent apoptosis in a manner that does not require prior cell cycle arrest and is not impeded by the overexpression of antiapoptotic proteins.

Based upon the ability of pivarubicin to circumvent multiple mechanisms of resistance against doxorubicin, we then examined the efficacy of pivarubicin against TNBC in comparison to doxorubicin. Figure 6A shows the results of in vitro cytotoxicity of pivarubicin and doxorubicin in two basal TNBC cell lines, MDA-MB-231 and SUM159[30]. Both cell lines exhibit a biphasic response to doxorubicin in MTT assays, with IC_{50} concentrations for MDA-MB-231 and SUM159 cells of 1 µM and 4 µM, respectively. However, the remaining

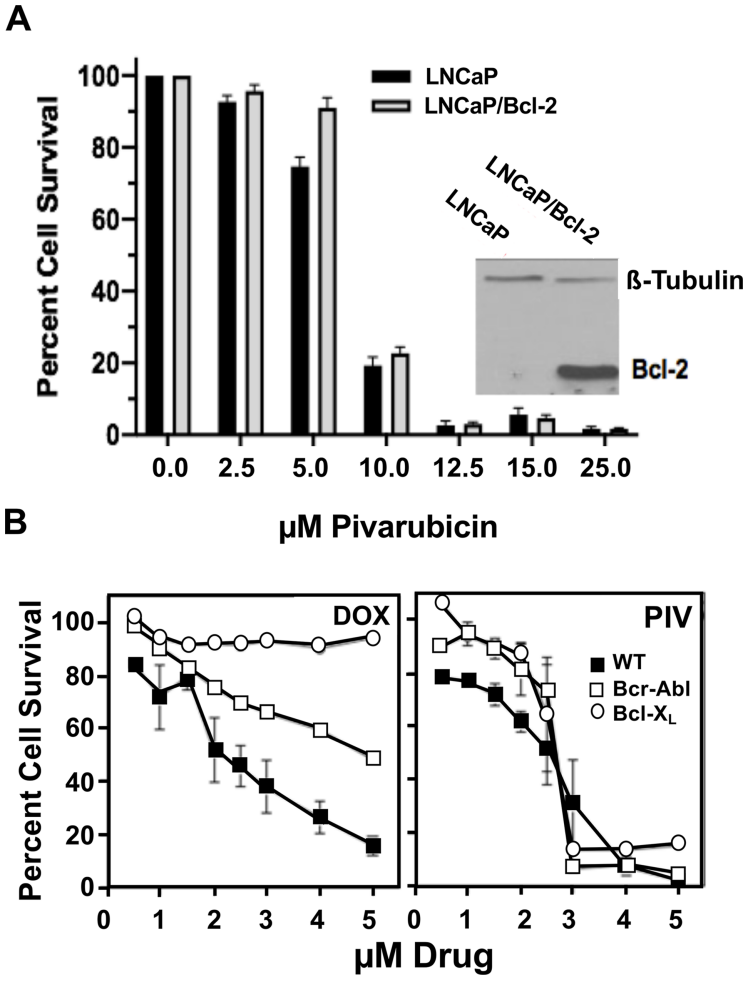

Figure 5. Pivarubicin circumvents multiple mechanisms of MDR. (A) LNCaP cells transfected with Bcl-2 expression vector were assessed for doxorubicin or pivarubicin cytotoxicity, compared to cells transfected with empty vectors. Cells were exposed to 5 µM drug for 1 h, washed, and further incubated for 72 h in drug-free medium. Viability was determined by the MTT assay. (B) Pivarubicin cytotoxicity in HL-60 cells transfected with Bcr-Abl or Bcl-X_L expression vectors were assessed for doxorubicin or pivarubicin cytotoxicity and compared as described for (A). Each datum point represents the mean and standard error of at least three independent determinations.

cell subpopulations were significantly less sensitive to doxorubicin, ultimately shifting the IC_{90} concentrations to >20 µM in both cell lines. In contrast, the response to pivarubicin treatment was largely monophasic in both cell lines, with IC_{50} concentrations of 2.5 µM and 1.5 µM, and IC_{90} concentrations of 4.5 µM and 1.7 µM in MDA-MB-231 and SUM159 cells, respectively. Consistent with monolayer cell culture results, pivarubicin was significantly more effective than doxorubicin in preventing secondary tumorsphere formation by MDA-MB-231 cells, with complete inhibition with 2.5 µM pivarubicin, but only partial inhibition by 2.5 µM doxorubicin (Fig. 6B). Similar results were observed with SUM159 tumorspheres (not shown).

The superiority of pivarubicin over doxorubicin in our in vitro findings led us to investigate whether pivarubicin demonstrates therapeutic superiority in vivo using an orthotopic xenograft model of luminescent MDA-MB-231 cells (LM2) engrafted into the left and right inguinal mammary glands of female NSG mice. Once achieving a primary tumor volume of 150–190 mm^3, mice were randomized into three cohorts for treatment with the MTD of pivarubicin or doxorubicin, or the equivalent volume of vehicle per body weight.

The MTD of pivarubicin and doxorubicin, as determined in 8-week-old nontumor-bearing female NSG mice, was defined as the dose given IP (rapid push in 70% sterile saline, 15% EtOH, 15% Cremophor EL) once every 2 weeks (two doses) that produced a maximum reversible 20% decrease in mean body weight. Based on this criterion, the MTD for doxorubicin was 1.4 mg/kg (reversible mean weight loss of 22%). The MTD for pivarubicin was 26.6 mg/kg, producing a reversible mean weight loss of 20%.

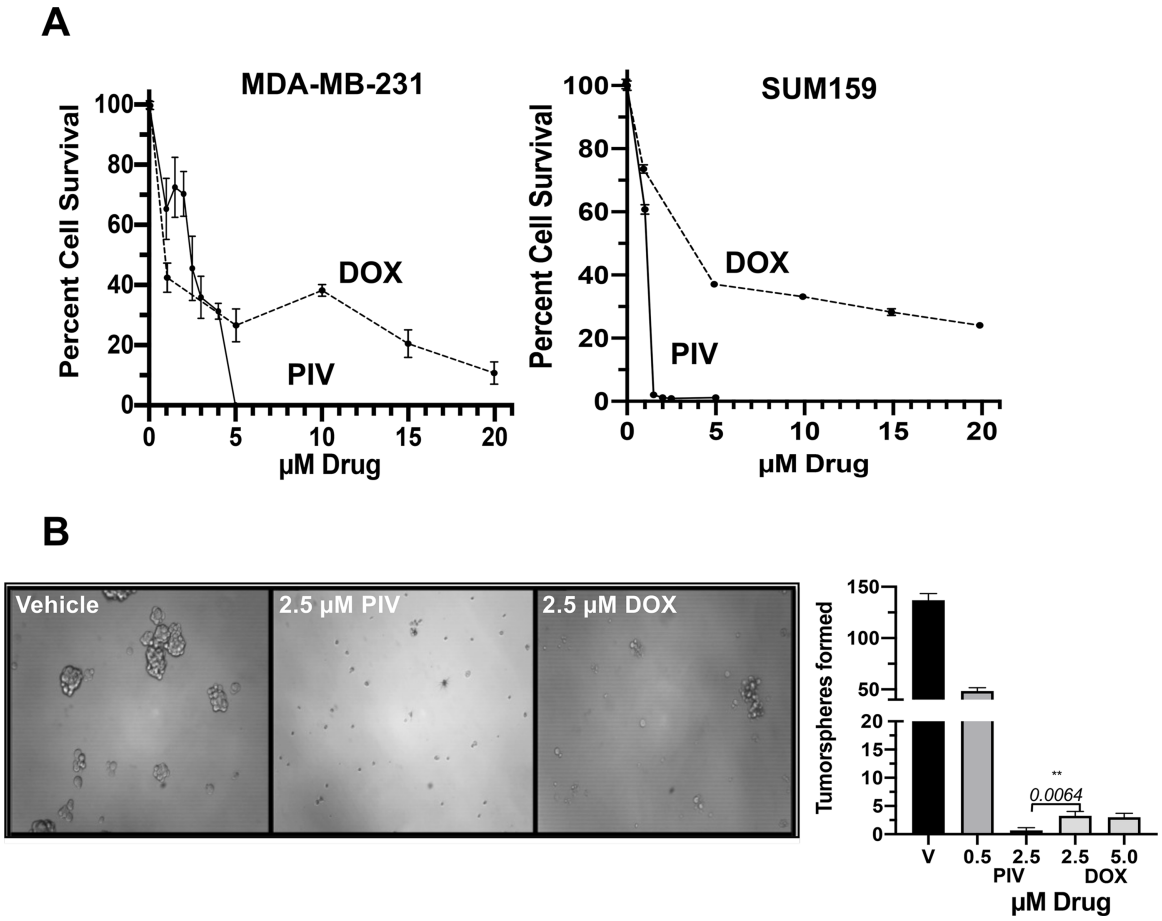

Figure 6. Pivarubicin is more cytotoxic than doxorubicin against triple-negative breast cancer (TNBC) monolayer cells. (A) MDA-MB-231 and SUM-159 cells were maintained under adherent monolayer growth conditions. Upon reaching 50% confluency, cells were treated for 48 h with the dose range of doxorubicin or pivarubicin as indicated. Cell viability was corrected for death observed in vehicle-only-treated cells (<1% ethanol final well concentration). (B) MDA-MB-231 monolayer culture was plated at 6,500 cells per well into a 24-well ultralow adhesion dish in tumorsphere medium with either vehicle, doxorubicin (DOX), or pivarubicin (PIV) and cultured for up to 7 days prior to obtaining digital images. Bar graph represents the mean number of tumorspheres greater than 50 mm in diameter/well ($n > 3$).

Primary LM2 tumors treated with either a single IP dose of 1.4 mg/kg or a subsequent escalated dose of 1.6 mg/kg of doxorubicin 14 days later failed to exhibit reduced growth compared with vehicle treatment, as indicated by in vivo tumor volume measurements during treatment (Fig. 7A) or endpoint volume (Fig. 7B) and weight (Fig. 7C) determinations of excised tumors. Luminescence comparison of doxorubicin- and vehicle-treated primary tumors (Fig. 7D) demonstrated similar flux, suggesting that both groups of tumors had comparable quantities of live cells. Further dosing with doxorubicin was precluded by excessive and irreversible weight loss in tumor-bearing mice.

In contrast, a single IP dose of pivarubicin at 26.6 mg/kg produced a mean 40% decrease in tumor volume compared with the mean volume prior to drug administration, indicating not only inhibition of further tumor growth but also regression of tumor mass. This is compared with a 3.5-fold increase in tumor volume in mice treated with vehicle alone (Fig. 8A). As opposed to nontumor-bearing NSG mice, a single MTD of pivarubicin in tumor-bearing NSG mice resulted in a poorly reversible 20% mean weight loss, precluding additional dosing. As a consequence, we performed a second, independent dosing experiment in which tumor-bearing NSG mice were treated with pivarubicin in two doses of 16.5 mg/kg IP at a 2-week interval (Fig. 8B), after which the primary tumors were removed, then measured for volume (Fig. 8C) and weight (Fig. 8D). Endpoint measurements indicated that two rounds of 16.5 mg/kg of pivarubicin produced a 50% decrease in tumor volume and 40% decrease in tumor weight compared with vehicle treatment.

Taken together, these results indicate that while the MTD of doxorubicin is subtherapeutic against a rapidly

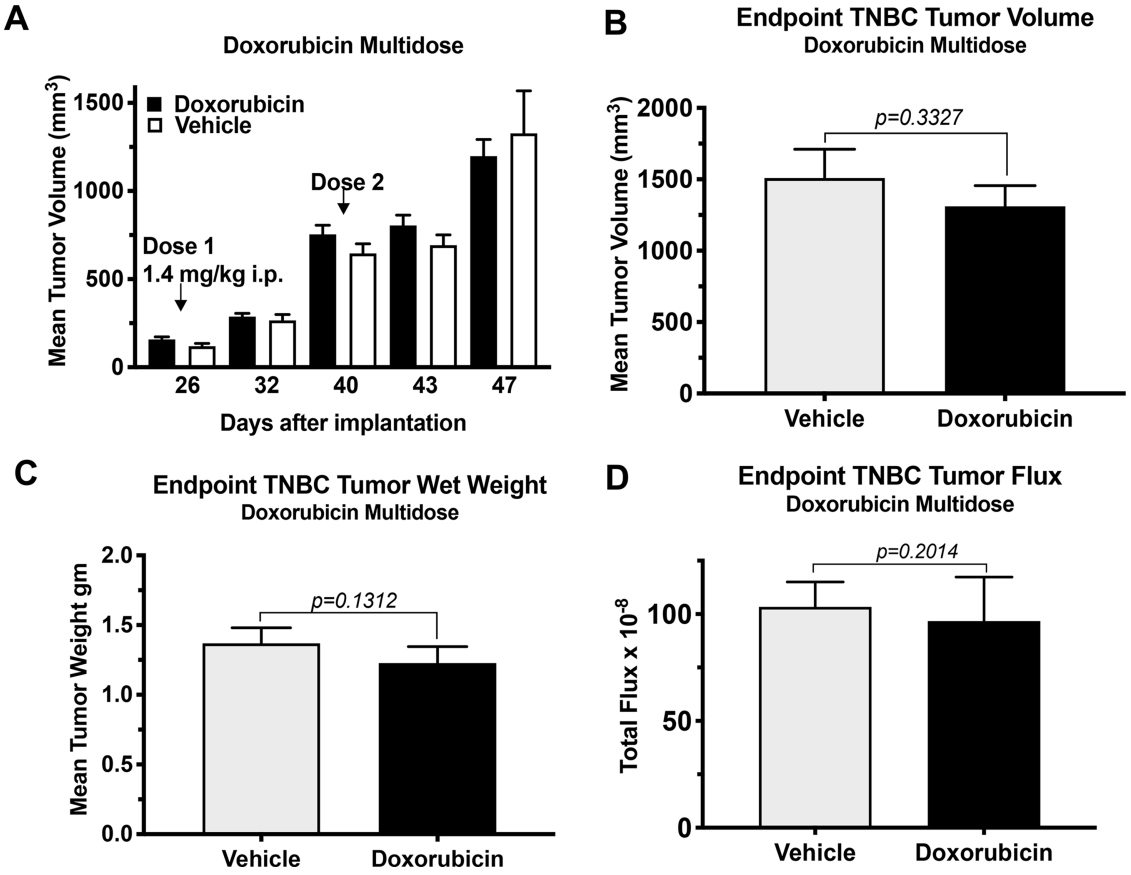

Figure 7. Doxorubicin treatment of TNBC-bearing NSG mice. (A) LM2 cells were implanted into the 4R and 4L cleared mammary fat pads of female NSG mice and permitted to proliferate for 26 days until a tumor volume range of 125–190 mm^3 was reached based on caliper measurements. Doxorubicin was administered IP rapid push in 70% sterile saline, 15% EtOH, 15% Cremophor EL at 14-day intervals, with tumor volumes measured at indicated days postimplantation. Dosing was suspended at 47 days due to tumor size. At endpoint, mice were euthanized and primary tumors resected for volume (B), weight (C), and luminescence (D) measurements. Endpoint results are expressed as the mean ± standard error of 10 mice per group. Statistical significance was determined by the Wilcoxon rank-sum test.

growing and aggressive human TNBC orthotopic xenograft, pivarubicin not only inhibited tumor proliferation but also produced tumor regression.

Given the limitation of doxorubicin in the treatment of tumors due to irreversible cardiotoxicity as a consequence of the total cumulative dose of drug, it was next determined whether pivarubicin produced evidence of cardiotoxic damage at the total dose of drug administered to NSG mice that produced tumor growth inhibition. Histological evidence of ventricular damage in hearts of drug- or vehicle-treated NSG mice was assessed using the Bertazzoli test, originally designed to assess doxorubicin-induced cardiomyocyte damage[29]. Analyses were performed on hearts from two independent experiments: 1) hearts that were excised at dosing endpoint from tumor-bearing NSG mice receiving two IP doses of pivarubicin at 16.5 mg/kg, doxorubicin at 1.4 mg/kg then 1.6 mg/kg, and an equivalent volume of vehicle alone and 2) nontumor-bearing female NSG mice receiving three IP doses of pivarubicin at 16.5 mg/kg, doxorubicin at 1.4 mg/kg then 1.6 mg/kg × 2, and an equivalent volume of vehicle alone at 2-week intervals.

As shown in Table 2, nontumor-bearing mice ($n = 9$) given a cumulative dose of pivarubicin that was demonstrated to inhibit primary TNBC tumor growth exhibited no evidence of histologic damage to ventricular cardiomyocytes, as measured by both severity of damage to individual cells and extent of the lesion. Similarly, 9/10 hearts from tumor-bearing NSG mice treated with pivarubicin at a cumulative tumor growth inhibitory dose showed no evidence of myocardial damage. In contrast, doxorubicin treatment of nontumor-bearing mice at its subtherapeutic MTD resulted in detectable damage to cardiomyocytes in 4/9 hearts, based on severity. Doxorubicin-treated tumor-bearing mice exhibited less cardiotoxicity (2/9 hearts), but received a lower cumulative dose than nontumor-

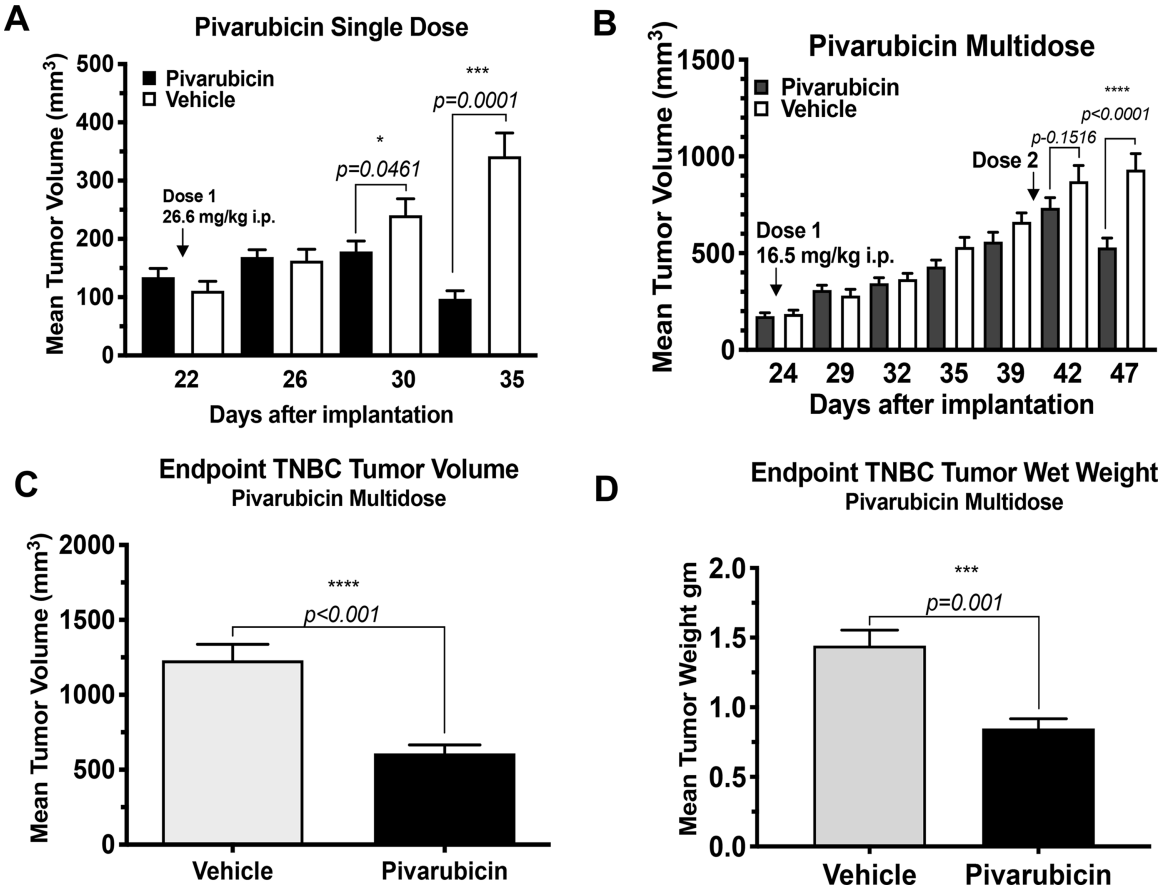

Figure 8. Pivarubicin treatment of TNBC-bearing NSG mice. LM2 cells were implanted into the 4R and 4L cleared mammary fat pads of female NSG mice and permitted to proliferate for 22–24 days until a tumor volume range of 125–190 mm^3 was reached based on caliper measurements. Pivarubicin was administered IP rapid push in 70% sterile saline, 15% EtOH, 15% Cremophor EL as either a single dose at 26.6 mg/kg (A) or in two 16.5-mg/kg doses at a 14-day interval (B) with tumor volumes measured at indicated days postimplantation. Dosing was suspended at 47 days due to tumor size in vehicle-treated mice. At endpoint, mice were euthanized and primary tumors resected for volume (C) and weight (D) measurements. Results are expressed as the mean ± standard error of 10 mice per group. Statistical significance was determined by the Wilcoxon rank-sum test.

Table 2. Cardiotoxicity Analysis of Nontumor-Bearing and Triple-Negative Breast Cancer-Bearing Mice

	Nontumor Bearing			Tumor Bearing		
	Vehicle	DOX	PIV	Vehicle	DOX	PIV
Severity						
0	7/9	5/9	9/9	13/18	7/9	9/10
0.5	0/9	0/9	0/9	0/18	0/9	0/10
1.0	2/9	4/9	0/9	5/18	2/9	1/10
Total score						
0	7/9	7/9	9/9	14/18	8/9	9/10
0.5	2/9	2/9	0/9	4/18	1/9	0/10
1.0	0/9	0/9	0/9	0/18	0/9	1/10

Values are number of hearts with indicated score per total number evaluated. DOX, doxorubicin; PIV, pivarubicin.

bearing mice. Paradoxically, vehicle-treated mice from both experiments (tumor bearing, $n=18$; nontumor bearing, $n=10$) exhibited evidence of myocardial damage in 4/18 and 2/9 hearts, respectively. Figure 9 shows representative stained thin sections of ventricular cardiomyocytes from nontumor-bearing mouse hearts showing visible evidence of microvacuolization. These results indicate that at a cumulative dose that inhibits TNBC tumor growth, pivarubicin produces no detectable cardiac damage.

DISCUSSION

The design of more effective treatments for TNBC continues to be challenging, owing to the 1) absence of exploitable receptor targets, in contrast to ER^+/PR^+ and $HER2^+$ breast tumors, which limits options for targeted therapy[31], and 2) the emergence of refractory cancer cells possessing broad-spectrum resistance, which limits the efficacy of current chemotherapeutic agents[2]. By exploiting an alternative mechanistic strategy of foregoing the traditional targets of cytotoxic chemotherapy to directly trigger apoptosis via PKCd activation, we report here on the potential superiority of the functionally novel anthracycline, pivarubicin, over the standard-of-care drug, doxorubicin, in the treatment of TNBC. Against primary human MDA-MB-231 TNBC tumors in an orthotopic mouse model, doxorubicin failed to inhibit tumor growth, while pivarubicin not only inhibited growth but also produced tumor regression after a single administration of its MTD. Further, tumor growth inhibition was achieved without the detectable histological damage to ventricular cardiomyocytes often observed at therapeutic doses of doxorubicin in clinical settings, suggesting both improved antitumor efficacy and safety of pivarubicin.

Our current approach to improve chemotherapy with functionally novel anthracycline congeners has been previously successful. Valrubicin (Valstar®) is a cytoplasmic-targeted 14-*O*-acyl trifluoroacetyl anthracycline, designed and developed in-house[32], that is currently FDA approved for intravesicular administration for human superficial bladder carcinoma, as well as in the preclinical stages of development for the treatment of TNBC, psoriasis, and acne[33–35]. The pivarubicin congener, AD 198, is currently in preclinical development for canine osteosarcoma[36], while the mixed function hybrid anthracycline, AD 312[37], is undergoing clinical trials against canine B-cell lymphoma. AD 198 has been more extensively evaluated in terms of cytotoxic mechanisms, noncardiotoxicity, cardioprotection, and in vivo antitumor efficacy[12,13,17,38]. However, the hydrolytic lability of the valerate moiety of AD 198 to yield the functionally distinct congener, AD 288, is both an asset and a liability to antitumor activity. While the biotransformation of AD 198 to AD 288 confers a multifunctional characteristic to AD 198, AD 288 cytotoxicity is inhibited by mechanisms of resistance that do not impede AD 198 or pivarubicin resistance. The sustained stability of pivarubicin ensures a prolonged ability of the drug to remain active against tumor cells that are resistant to chemotherapy through increased expression of multidrug transport proteins or antiapoptotic Bcl-2 proteins, in contrast to AD 198[38]. Therefore, pivarubicin was selected as our drug of choice for further in vivo evaluation against TNBC.

Pivarubicin possesses unique structural and functional characteristics that promote rapid intracellular accumulation unaffected by P-glycoprotein overexpression and nonnuclear localization in the perinuclear cytoplasm. This unconventional localization of an anthracycline eliminates nuclear DNA damage and subsequent cell cycle arrest as requisite events for cell kill and results in direct activation of cytoplasmic PKCd, leading to mitochondrial-dependent apoptosis that is uninhibited by Bcl-2 overexpression. This latter characteristic is particularly significant in light of the high level of Bcl-2 expression in MDA-MB-231 cells observed by our labs (not shown), as well as by others[39–41] and can explain the improved antitumor efficacy of pivarubicin over doxorubicin. Bcl-2 expression impedes doxorubicin-induced apoptosis in TNBC cells[42] as well as in a variety of other tumor cell lines[43], but has no effect

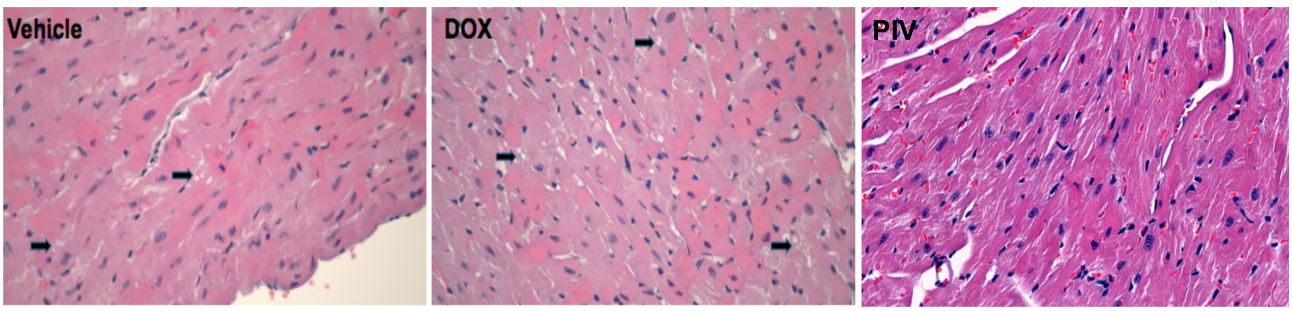

Figure 9. Representative stained thin sections: cardiotoxicity analysis of nontumor-bearing NSG mice. Images show evidence of microvacuolization (arrows) in both vehicle- and doxorubicin-treated mice.

on pivarubicin cytotoxicity. Growth of MDA-MB-231 cells in contact with extracellular matrix proteins has been reported to further enhance Bcl-2 expression, increasing resistance to doxorubicin[42]. Claudin-low TNBC tumor cells surviving in vivo after neoadjuvant therapy demonstrate the overexpression of both Myc and the antiapoptotic Bcl-2 family protein, Mcl-1, to cooperatively confer drug resistance[44] through enhanced mitochondrial oxidative phosphorylation to enhance cancer stem cell viability[45]. Given the ability of pivarubicin to circumvent the antiapoptotic effects of Bcl-2 family member proteins and the ability of the pivarubicin congener, AD 198, to inhibit Myc expression[46,47], it is likely that pivarubicin would be unaffected by the emergence of this mechanism of resistance.

Doxorubicin cytotoxicity is produced, in part, by inhibition of topoisomerase II DNA ligase activity, resulting in the accumulation of double-stranded breaks (DSBs), repairable largely by nonhomologous recombination[48]. Inactivating BRCA1/2 mutations, occurring in 20% of TNBC tumors, result in reduced DNA double-strand break (DSB) repair and increased tumor sensitivity to anthracyclines[4,49] and PARP-inhibitory drugs[2]. Breast cancer cell lines, such as MDA-MB-231, with normal BRCA but mutant p53 exhibit decreased sensitivity to DNA-damaging agents[50]. The cytoplasmic localization of pivarubicin and its targeting of C1b domain-containing enzymes, such as PKC and RacGRP, significantly reduce the influence of changes in DSB repair potential on drug cytotoxicity, in contrast to doxorubicin. Additionally, we have previously shown that pivarubicin cellular effects occur independently of ATM or p53 activities[51].

Resistance to anthracyclines and taxanes has also been established in TNBC cell lines through the expression of multidrug transport proteins MDR1 and MRP-1, -5, and -6[52,53], as has been extensively observed in a variety of human tumor cells exposed to these classes of drugs both in vitro and in vivo[54,55]. While MDA-MB-231 cells express P-gp or MRP only following selective pressure with anthracyclines and other cytotoxic drugs that are transport substrates[56], the ability of pivarubicin to circumvent transported-mediated resistance indicates its utility as a salvage therapy for refractory tumors as well as first-line therapy. However, the results presented in this study suggest that LM2 cells, which have not been specifically selected for drug resistance, respond rapidly to pivarubicin but not doxorubicin, pointing to the potential of pivarubicin as first-line treatment.

The precise mechanism of in vivo tumor growth inhibition by pivarubicin is not yet confirmed. While the cytotoxic action of pivarubicin is linked to PKCd-mediated activation of apoptosis, PKCd activity in MDA-MB-231 cells has been linked with the promotion of cell survival[57,58] and tumor cell migration through MAPK activation[59,60], but is also linked to cell cycle arrest and apoptosis through PKCd-dependent p21 or p27 activity[61,62]. We have previously reported with AD 198 that rapid apoptosis associated with AD 198-mediated PKCd activation in HL-60 cells occurs simultaneously with the phosphorylation of ERK1/2, STAT5, and Jun[14]. This suggests that while these anthracyclines have the ability to activate proliferative signaling in a PKC-dependent manner, proapoptotic signaling, nevertheless, predominates. Thus, in LM2 cells, the net effect of pivarubicin treatment is inhibition of tumor growth.

In addition to the limited efficacy of doxorubicin due to multiple mechanisms of multidrug resistance, the increased risk of irreversible cardiac damage by anthracycline therapy is well established and is an impediment to curative anthracycline-based therapy for cancer patients[63]. Compounding this risk is the established cardiotoxic potential of taxanes and alkylating agents[64], which are administered in combination with doxorubicin. As a consequence of the current impediments to curative anthracycline-based therapy, two distinct strategies have been adopted to improve treatment: modification of anthracycline delivery in combination with conventional agents, or identification and exploitation of novel targets in TNBC. Pegylated liposomal doxorubicin (PLD) has been proposed as an alternative for TNBC patients for whom further anthracycline treatment is contraindicated, based on the comparable antitumor efficacy and reduced cardiotoxic potential of PLD[31,65]. However, while PLD treatment resulted in reduced cardiotoxicity in TNBC patients as well as other, non-life-threatening adverse effects, there were no significant improvements in any therapeutic parameters compared with doxorubicin. As a consequence, PLD has been considered as only noninferior to doxorubicin in clinical trials[31].

As an alternative to the conventional mechanisms of action of DNA damage and mitotic spindle inhibition, a wide variety of new targets in TNBC are currently under evaluation in phases I–II clinical trials, including inhibitors of DNA repair enzymes (PARP), inhibitors of proliferative signaling components (mTOR, AKT, MEK), 3) immunomodulatory targets (PD-1), and hormone receptors (AR)[2,31]. While drugs that target these sites have resulted in pCR of 39% with bevacizumab (anti-VEGF) and up to 85% with pembrolizumab (PD-1 blocker) in early clinical trials, all targeted agents have been administered in combination with conventional agents, including doxorubicin to achieve therapeutic success[2].

While the curative potential of pivarubicin against TNBC is not yet firmly established, this proof-of-principle study suggests that TNBC tumor eradication with pivarubicin can be achieved with optimal dosing and scheduling. A bolus MTD of pivarubicin was clearly effective in reducing TNBC tumor volume, but with >20% mean

body weight loss that was poorly recoverable, but without accompanying morbidities, precluded further dosing to achieve additional tumor regression and eradication, as per animal care guidelines. This, combined with the highly aggressive and invasive nature of LM2 cells, with rapid and early spread to axillary lymph nodes, liver, and lungs[66] suggests that fractional dosing on a daily basis would be more pharmacologically and therapeutically advantageous, as we have previously observed with AD 198[38] and valrubicin (M. Israel, personal communication). We noted an apparent difference in MTD for pivarubicin in tumor-bearing versus nontumor-bearing mice, whereas the doxorubicin MTD remained unchanged. This discrepancy points to the need for a more comprehensive understanding of pivarubicin pharmacokinetics in tumor- versus nontumor-bearing animals as well as further investigation into optimal dosing regimens for pivarubicin, both of which are planned.

The absence of histological evidence of cardiotoxicity at therapeutic doses of pivarubicin, including microvacuolization (Table 2, Fig. 9) and myofibrillar loss (not shown), would not necessarily be predictable, given the multiple possible mechanisms of anthracycline-induced cardiotoxicity in addition to the generation of ROS from the anthraquinone ring structure[67–69]. Indeed, preliminary morphological analysis revealed ventricular wall thinning and cavity enlargement in some pivarubicin-treated hearts from tumor-bearing mice described in Figure 8 and enlargement of hearts from nontumor-bearing mice treated with pivarubicin and to a lesser extent with doxorubicin (not shown). However, based on the close functional similarity of pivarubicin to AD 198 and our previous observations that AD 198 is both noncardiotoxic and functionally cardioprotective through activation of PKCe in rodent cardiomyocytes despite generation of ROS comparable to doxorubicin[17,18], pivarubicin possesses the potential to be noncardiotoxic. It is worth noting in our results that vehicle treatment, alone, produced microvacuolization similar to doxorubicin/vehicle and greater than pivarubicin/vehicle treatment. While Cremophor EL/ethanol has been previously reported to produce a decrease in mitochondrial respiration[70], there have been no reports of Cremophor EL/ethanol-induced microvacuolization in cardiomyocytes in either our laboratories or elsewhere. Given the marginal histological evidence of cardiotoxicity with doxorobucin in our studies, the differences in cardiotoxicity between vehicle and doxorubicin may not be significant. The nearly complete absence of microvacuolization in pivarubicin/vehicle-treated hearts could be a consequence of predicted cardioprotective action of pivarubicin, but this remains to be established, as does the structural and functional cardiac effects of pivarubicin through a more in-depth analysis.

In summary, the initial success in demonstrating the potential superiority of pivarubicin over doxorubicin against human TNBC in a mouse xenograft model is the first step in the clinical development of pivarubicin as a safer and more effective replacement for doxorubicin in TNBC combination chemotherapy. This preclinical proof-of-principle will be followed up by pivarubicin dosing optimization analysis of pivarubicin efficacy against TNBC metastases in our human TNBC xenograft model as a prelude to eventual clinical development.

ACKNOWLEDGMENTS: All in vitro studies were supported by NCI R01CA100093 (to L.L.), while in vivo studies and synthesis of pivarubicin were supported through an unrestricted gift from Cumberland Pharmaceuticals, Inc. (to L.L.), NCI R01CA138488 (to T.N.S.) and the Methodist/West Cancer Center Support Fund. We are indebted to Dr. Mervyn Israel for the design of pivarubicin and AD 198, and Mila Savranskaya and Bethany Larkin are thanked for their excellent technical assistance. The authors declare no conflicts of interest.

REFERENCES

1. O'Reilly EA, Gubbins L, Sharma S, Tully R, Guang MH, Weiner-Gorzel K, McCaffrey J, Harrison M, Furlong F, Kell M, McCann A. The fate of chemoresistance in triple negative breast cancer (TNBC). BBA Clin. 2015;3:257–75.
2. Omarini C, Guaitoli G, Pipitone S, Moscetti L, Cortesi L, Cascinu S, Piacentini F. Neoadjuvant treatments in triple-negative breast cancer patients: Where we are now and where we are going. Cancer Manag Res. 2018;10:91–103.
3. Sharma P. Update on the treatment of early-stage triple-negative breast cancer. Curr Treat Options Oncol. 2018;19:22.
4. Jhan JR, Andrechek ER. Triple-negative breast cancer and the potential for targeted therapy. Pharmacogenomics 2017;18:1595–609.
5. Liedtke C, Mazouni C, Hess, KR, André, F, Tordai A, Mejia JA, Symmans WF, Gonzalez-Angulo AM, Hennessy B, Green M, Cristofanilli M, Hortobagyi GN, Pusztai L. Response to neoadjuvant therapy and long-term survival in patients with triple-negative breast cancer. J Clin Oncol. 2008;26:1275–81.
6. Fournier MV, Goodwin EC, Chen J. Obenauer JC, Tannenbaum SH, Brufsky AM. A Predictor of pathological complete response to neoadjuvant chemotherapy stratifies triple negative breast cancer patients with high risk of recurrence. Sci Rep. 2019;9:14863.
7. Yeh ET, Bickford CL. Cardiovascular complications of cancer therapy: Incidence, pathogenesis, diagnosis, and management. J Am Coll Cardiol. 2009;53:2231–47.
8. Menna P, Salvatorelli E, Minotti G. Cardiotoxicity of antitumor drugs. Chem Res Toxicol. 2008;21:978–89.
9. Lothstein L, Israel M, Sweatman TW. Anthracycline drug targeting: Cytoplasmic versus nuclear—A fork in the road. Drug Resist Update 2001;4:169–77.
10. Roaten JB, Kazanietz MG, Caloca MJ, Bertics PJ, Lothstein L, Parrill AL, Israel M, Sweatman TW. Interaction of the novel anthracycline antitumor agent *N*-benzyladriamycin-14-valerate with the C1-regulatory domain of protein kinase C: Structural requirements, isoform specificity, and correlation with drug cytotoxicity. Mol Cancer Ther. 2002;1:483–92.
11. Roaten JB, Kazanietz MG, Sweatman TW, Lothstein L, Israel M, Parrill AL: Molecular models of *N*-benzyladriamycin-

14-valerate (AD 198) in complex with the phorbol ester-binding C1b domain of protein kinase C-delta. J Med Chem. 2001;44:1028–34.
12. Barrett CM, Lewis FL, Roaten JB, Sweatman TW, Israel M, Cleveland JL, Lothstein L. Novel extranuclear-targeted anthracyclines override the antiapoptotic functions of Bcl-2 and target protein kinase C pathways to induce apoptosis. Mol Cancer Ther. 2002;1:469–81.
13. Lothstein L, Savranskaya L, Barrett CM, Israel M, Sweatman TW. *N*-Benzyladriamycin-14-valerate (AD 198) activates protein kinase C-delta holoenzyme to trigger mitochondrial depolarization and cytochrome c release independently of permeability transition pore opening and Ca^{2+} influx. Anticancer Drugs 2006;17:495–502.
14. Lothstein L, Savranskaya L, Sweatman TW. *N*-Benzyladriamycin-14-valerate (AD 198) cytotoxicity circumvents Bcr-Abl anti-apoptotic signaling in human leukemia cells and also potentiates imatinib cytotoxicity. Leuk Res. 2007;31:1085–95.
15. He Y, Liu J, Durrant D, Yang HS, Sweatman T, Lothstein L, Lee RM. *N*-benzyladriamycin-14-valerate (AD 198) induces apoptosis through protein kinase C-delta-induced phosphorylation of phospholipid scramblase 3. Cancer Res. 2005;65:10016–23.
16. He Y, Liu J, Grossman D, Durrant D, Sweatman T, Lothstein L, Epand RF, Epand RM, Lee RM. Phosphorylation of mitochondrial phospholipid scramblase 3 by protein kinase C-delta induces its activation and facilitates mitochondrial targeting of tBid. J Cell Biochem. 2007;101:1210–21.
17. Hofmann PA, Israel M, Koseki Y, Laskin J, Gray J, Janik A, Sweatman TW, Lothstein L. *N*-Benzyladriamycin-14-valerate (AD 198): A non-cardiotoxic anthracycline that is cardioprotective through PKC-epsilon activation. J Pharmacol Exp Ther. 2007;323:658–64.
18. Cai C, Lothstein L, Morrison RR, Hofmann PA. Protection from doxorubicin-induced cardiomyopathy using the modified anthracycline *N*-benzyladriamycin-14-valerate (AD 198). J Pharmacol Exp Ther. 2010;335:223–30.
19. Lothstein L, Suttle DP, Roaten JB, Koseki Y, Israel M, Sweatman TW. Catalytic inhibition of DNA topoisomerase II by *N*-benzyladriamycin (AD 288). Biochem Pharmacol. 2000;60:1621–8.
20. Lothstein L, Rodrigues PJ, Sweatman TW, Israel M. Cytotoxicity and intracellular biotransformation of *N*-benzyladriamycin-14-valerate (AD 198) are modulated by changes in 14-*O*-acyl chain length. Anticancer Drugs 1998;9:58–66.
21. Israel M, Idriss JM, Koseki Y, Khetarpal VK. Comparative effects of adriamycin and DNA-non-binding analogues on DNA, RNA, and protein synthesis *in vitro*. Cancer Chemother Pharmacol. 1987;20:277–84.
22. Beck WT, Mueller TJ, Tanzer LR. Altered surface membrane glycoproteins in vinca alkaloid-resistant human leukemic lymphoblasts. Cancer Res.1979;39:2070–6.
23. Conter V, Beck WT. Acquisition of multiple drug resistance by CCRF-CEM cells selected for different degrees of resistance to vincristine. Cancer Treat Rep. 1984;68:831–9.
24. Lu X, Yan CH, Yuan M, Wei Y, Hu G, Kang Y. *In vivo* dynamics and distinct functions of hypoxia in primary tumor growth and organotropic metastasis of breast cancer. Cancer Res. 2010;70:3905–14.
25. Yoshida K, Wang HG, Miki Y, Kufe D. Protein kinase Cdelta is responsible for constitutive and DNA damage-induced phosphorylation of Rad9. EMBO J. 2003;22:1431–41.
26. Sweatman TW, Seshadri R, Israel M. Pharmacology of *N*-benzyladriamycin-14-valerate in the rat. Cancer Chemother Pharmacol. 1999;43:419–26.
27. Sweatman TW, Israel M. Comparative metabolism and elimination of adriamycin and 4'-epiadriamycin in the rat. Cancer Chemother Pharmacol. 1987;19:201–6.
28. Mosmann T. Rapid colorimetric assay for cellular growth and survival: Application to proliferation and cytotoxicity assays. J Immunol Methods 1983;65:55–63.
29. Bertazzoli C, Bellini O, Magrini U, Tosana MG. Quantitative experimental evaluation of adriamycin cardiotoxicity in the mouse. Cancer Treat Rep. 1979;63:1877–83.
30. Holliday DL, Speirs V. Choosing the right cell line for breast cancer research. Breast Cancer Res. 2011;13:215.
31. Zeichner SB, Terawaki H, Gogineni K. A review of systemic treatment in metastatic triple-negative breast cancer. Breast Cancer (Auckl) 2016;10:25–36.
32. Sweatman TW, Parker RF, Israel M: Pharmacologic rationale for intravesical *N*-trifluoroacetyladriamycin-14-valerate (AD 32): A preclinical study. Cancer Chemother Pharmacol. 1991;28:1–6.
33. Hauge E, Christiansen H, Rosada C, de Darkó E, Dam TN, Stenderup K: Topical valrubicin application reduces skin inflammation in murine models. Br J Dermatol. 2012;167:288–95.
34. Rottboell L, de Foenss S, Thomsen K, Christiansen H, Andersen SM, Dam TN, Rosada C, Stenderup K. Exploring valrubicin's effect on Propionibacterium acnes-induced skin inflammation *in vitro* and *in vivo*. Dermatol Reports 2015;7:6246.
35. Johnson R, Sabnis N, Sun X, Ahluwalia R, Lacko AG. SR-B1-targeted nanodelivery of anti-cancer agents: A promising new approach to treat triple-negative breast cancer. Breast Cancer 2017;9:383–92.
36. Rathore K, Cekanova M. A novel derivative of doxorubicin, AD198, inhibits canine transitional cell carcinoma and osteosarcoma cells in vitro. Drug Des Devel Ther. 2015;9:5323–35.
37. Pawlik CA, Israel M, Sweatman TW, Lothstein L. Cellular resistance against the novel hybrid anthracycline *N*-(2-chloroethyl)-*N*-nitrosoureidodaunorubicin (AD 312) is mediated by combined altered topoisomerase II and O6-methylguanine-DNA methyltransferase activities. Oncol Res. 1998;10:209–17.
38. Ganapathi R, Grabowski D, Sweatman TW, Seshadri R, Israel M. *N*-Benzyladriamycin-14-valerate versus progressively doxorubicin-resistant murine tumours: Cellular pharmacology and characterisation of cross-resistance *in vitro* and *in vivo*. Br J Cancer 1989;60:819–26.
39. Huang WC, Su HH, Fang LW, Wu SJ, Liou CJ. Licochalcone A inhibits cellular motility by suppressing E-cadherin and MAPK signaling in breast cancer. Cells 2019;8:E218.
40. Hwang E, Hwang SH, Kim J, Park JH, Oh S, Kim YA, Hwang KT. ABT-737 ameliorates docetaxel resistance in triple negative breast cancer cell line. Ann Surg Treat Res. 2018;95:240–8.
41. Inao T, Iida Y, Moritani T, Okimoto T, Tanino R, Kotani H, Harada M. Bcl-2 inhibition sensitizes triple-negative human breast cancer cells to doxorubicin. Oncotarget 2018;9:25545–56.
42. Lovitt CJ, Shelper TB, Avery VM. Doxorubicin resistance in breast cancer cells is mediated by extracellular matrix proteins. BMC Cancer 2018;18:41.

43. Campbell KJ, Tait SWG. Targeting Bcl-2 regulated apoptosis in cancer. Open Biol. 2018;8:180002.
44. Balko JM, Giltnane JM, Wang K, Schwarz LJ, Young CD, Cook RS, Owens P, Sanders ME, Kuba MG, Sánchez V, Kurupi R, Moore PD, Pinto JA, Doimi FD, Gómez H, Horiuchi D, Goga A, Lehmann BD, Bauer JA, Pietenpol JA, Ross JS, Palmer GA, Yelensky R, Cronin M, Miller VA, Stephens PJ, Arteaga CL. Molecular profiling of the residual disease of triple-negative breast cancers after neoadjuvant chemotherapy identifies actionable therapeutic targets. Cancer Discov. 2014;4:232–45.
45. Lee KM, Giltnane JM, Balko JM, Schwarz LJ, Guerrero-Zotano AL, Hutchinson KE, Nixon MJ, Estrada MV, Sánchez V, Sanders ME, Lee T, Gómez H, Lluch A, Pérez-Fidalgo JA, Wolf MM, Andrejeva G, Rathmell JC, Fesik SW, Arteaga CL. MYC and MCL1 cooperatively promote chemotherapy-resistant breast cancer stem cells via regulation of mitochondrial oxidative phosphorylation. Cell Metab. 2017;26:633–47.
46. Edwards SK, Moore CR, Liu Y, Grewal S, Covey LR, Xie P. *N*-Benzyladriamycin-14-valerate (AD 198) exhibits potent anti-tumor activity on TRAF3-deficient mouse B lymphoma and human multiple myeloma. BMC Cancer 2013;13:481.
47. Pandey S, Bourn J, Cekanova M. Mutations of p53 decrease sensitivity to the anthracycline treatments in bladder cancer cells. Oncotarget 2018;9:28514–31.
48. Pommier Y, Leo E, Zhang H, Marchand C. DNA topoisomerases and their poisoning by anticancer and antibacterial drugs. Chem Biol. 2010;17:421–33.
49. Wang C, Zhang J, Wang Y, Ouyang T, Li J, Wang T, Fan Z, Fan T, Lin B, Xie Y. Prevalence of BRCA1 mutations and responses to neoadjuvant chemotherapy among BRCA1 carriers and non-carriers with triple-negative breast cancer. Ann Oncol. 2015;26:523–8.
50. O'Connor PM, Jackman J, Bae I, Myers TG, Fan S, Mutoh M, Scudiero DA, Monks A, Sausville EA, Weinstein JN, Friend S, Fornace AJ Jr, Kohn KW. Characterization of the p53 tumor suppressor pathway in cell lines of the National Cancer Institute anticancer drug screen and correlations with the growth-inhibitory potency of 123 anticancer agents. Cancer Res. 1997;57:4285–300.
51. Bilyeu JD, Panta GR, Cavin LG, Barrett CM, Turner EJ, Sweatman TW, Israel M, Lothstein L, Arsura M. Circumvention of nuclear factor kappaB-induced chemoresistance by cytoplasmic-targeted anthracyclines. Mol Pharmacol. 2004;65:1038–47.
52. Zhang LH, Yang AJ, Wang M, Liu W, Wang CY, Xie XF, Chen X, Dong JF, Li M. Enhanced autophagy reveals vulnerability of P-gp mediated epirubicin resistance in triple negative breast cancer cells. Apoptosis 2016;21:473–88.
53. Boichuk S, Galembikova A, Sitenkov A, Khusnutdinov R, Dunaev P, Valeeva E, Usolova N. Establishment and characterization of a triple negative basal-like breast cancer cell line with multi-drug resistance. Oncol Lett. 2017;14:5039–45.
54. Chung FS, Santiago JS, Jesus MF, Trinidad CV, See MF. Disrupting P-glycoprotein function in clinical settings: What can we learn from the fundamental aspects of this transporter? Am J Cancer Res. 2016;6:1583–98.
55. Zhang YK, Wang YJ, Gupta P, Chen ZS. Multidrug resistance proteins (MRPs) and cancer therapy. AAPS J.2015;17:802–12.
56. Kopecka J, Rankin GM, Salaroglio IC, Poulsen SA, Riganti C.P-glycoprotein mediated chemoresistance is reversed by carbonic anhydrase XII inhibitors. Oncotarget 2016;7:85861–75.
57. McCracken MA, Miraglia LJ, McKay RA, Strobl JS. Protein kinase C delta is a prosurvival factor in human breast tumor cell lines. Mol Cancer Ther. 2003;2:273–81.
58. Chauvin L, Goupille C, Blanc C, Pinault M, Domingo I, Guimaraes C, Bougnoux P, Chevalier S, Mahéo K. Long chain n-3 polyunsaturated fatty acids increase the efficacy of docetaxel in mammary cancer cells by downregulating Akt and PKCε/δ-induced ERK pathways. Biochim Biophys Acta 2016;1861:380–90.
59. Zuo Y, Wu Y, Chakraborty C. Cdc42 negatively regulates intrinsic migration of highly aggressive breast cancer cells. J Cell Physiol. 2012;227:1399–407.
60. Chen P, Lu N, Ling Y, Chen Y, Hui H, Lu Z, Song X, Li Z, You Q, Guo Q. Inhibitory effects of wogonin on the invasion of human breast carcinoma cells by downregulating the expression and activity of matrix metalloproteinase-9. Toxicology 2011;282:122–8.
61. Shanmugam M, Krett NL, Maizels ET, Murad FM, Rosen ST, Hunzicker-Dunn M. A role for protein kinase C delta in the differential sensitivity of MCF-7 and MDA-MB 231 human breast cancer cells to phorbol ester-induced growth arrest and p21 (WAFI/CIP1) induction. Cancer Lett. 2001;172:43–53.
62. Vucenik I, Ramakrishna G, Tantivejkul K, Anderson LM, Ramljak D. Inositol hexaphosphate (IP6) blocks proliferation of human breast cancer cells through a PKCdelta-dependent increase in p27Kip1 and decrease in retinoblastoma protein (pRb) phosphorylation. Breast Cancer Res Treat. 2005;91:35–45.
63. Bird BR, Swain SM. Cardiac toxicity in breast cancer survivors: Review of potential cardiac problems. Clin Cancer Res. 2008;14:14–24.
64. Babiker HM, McBride A, Newton M, Boehmer LM, Drucker AG, Gowan M, Cassagnol M, Camenisch TD, Anwer F, Hollands JM. Cardiotoxic effects of chemotherapy: A review of both cytotoxic and molecular targeted oncology therapies and their effect on the cardiovascular system. Crit Rev Oncol Hematol. 2018;126:186–200.
65. Lien MY, Liu LC, Wang HC, Yeh MH, Chen CJ, Yeh SP, Bai LY, Liao YM, Lin CY, Hsieh CY, Lin CC, Li LY, Lin PH, Chiu CF. Safety and efficacy of pegylated liposomal doxorubicin-based adjuvant chemotherapy in patients with stage I-III triple-negative breast cancer. Anticancer Res. 2014;34:7319–26.
66. Chavez KJ, Garimella SV, Lipkowitz S. Triple negative breast cancer cell lines: One tool in the search for better treatment of triple negative breast cancer. Breast Dis. 2010;32:35–48.
67. Renu K, V G A, P B TP, Arunachalam S. Molecular mechanism of doxorubicin-induced cardiomyopathy—An update. Eur J Pharmacol. 2018;818:241–53.
68. Nitiss KC, Nitiss JL. Twisting and ironing: Doxorubicin cardiotoxicity by mitochondrial DNA damage. Clin Cancer Res. 2014;20:4737–9.
69. Zhang S, Liu X, Bawa-Khalfe T, Lu LS, Lyu YL, Liu LF, Yeh ET. Identification of the molecular basis of doxorubicin-induced cardiotoxicity. Nat Med. 2012;18:1639–42.
70. Sanchez H, Zoll J, Bigard X, Veksler V, Mettauer B, Lampert E, Lonsdorfer J, Ventura-Clapier R. Effect of cyclosporin A and its vehicle on cardiac and skeletal muscle mitochondria: Relationship to efficacy of the respiratory chain. Br J Pharmacol. 2001;133:781–8.